Low Loss Polycrystalline Silicon Waveguides and Devices for Multilayer On-Chip Optical Interconnects

David Kwong*[a], Amir Hosseini[b], John Covey[a], Yang Zhang[a], Xiaochuan Xu[a] and Ray T. Chen[a]
[a]Microelectronics Research Center, University of Texas at Austin, 10100 Burnet Rd, Bldg 160, Austin, Texas 78758
[b]Omega Optics Inc., 10306 Sausalito Drive, Austin, TX, USA 78759
*david.kwong@utexas.edu, raychen@uts.cc.utexas.edu;

ABSTRACT

We have investigated the feasibility of multimode polysilicon waveguides to demonstrate the suitability of polysilicon as a candidate for multilayer photonic applications. Solid Phase Crystallization (SPC) with a maximum temperature of 1000°C is used to create polysilicon on thermally grown SiO_2. We then measure the propagation losses for various waveguide widths on both polysilicon and crystalline silicon platforms. We find that as the width increases for polysilicon waveguides, the propagation loss decreases similar to crystalline silicon waveguides. The difference in loss between the two platforms for a given waveguide width is due to the scattering from the polysilicon grain boundaries, which excites higher order modes. Depending on the waveguide width, these modes either propagate as higher order modes or are lost as radiation modes. Due to their different propagation constants, the presence of higher order modes is confirmed using sub-wavelength grating couplers. At a waveguide width of 10μm, polysilicon and crystalline silicon waveguides have propagation losses of 0.56dB/cm and 0.31dB/cm, respectively, indicating there is little bulk absorption from the polysilicon. This propagation loss is the lowest for polysilicon demonstrated to date. Modal conversion in multimode waveguides by polysilicon grain boundary scattering are investigated using a sub-wavelength grating coupler and discussed. These results vindicate the use of polysilicon waveguides of varying widths in photonic integrated circuits.

Keywords: Silicon photonics, optical interconnects, waveguides, polycrystalline silicon, grating coupler, MMI

1. INTRODUCTION

On-chip photonic networks are a promising solution for the interconnect bottleneck in high performance microelectronics. Crystalline silicon-on-insulator (SOI) is the most commonly used photonics platform due to its large index contrast with silicon dioxide (Δn~2.02), which enables submicron waveguides and small bending radii. In addition, SOI exhibits excellent material properties such as low bulk absorption at telecom wavelengths and high electronic carrier mobility. While crystalline SOI is the most desirable, photonic devices would be restricted to the electronic layer. Furthermore, silicon photonics requires a thick Buried Oxide (BOX) layer (typically a few micrometers) for optical isolation from the substrate, but SOI for electronics requires a thin oxide layer ranging from tens to hundreds of nanometers to allow thermal flow into the substrate [1]. Although it has been shown that SOI for electronics can also be used for photonics [2], it comes generally at the cost of more real estate and adds greater complexity and cost to the standard CMOS fabrication process. A multi-layer platform would enable photonic device versatility, as footprint and separation issues are mitigated.

In order to maximize such a platform's design flexibility, CMOS compatible silicon deposition methods are strongly desired. As it is not currently possible to deposit crystalline silicon, alternative materials must be considered. Silicon nitride is a low loss material that has been used for multilayer photonic integration [1], but its lower index contrast increases device footprint, and it also lacks any mechanism for high-speed modulation, limiting nitride to either passive devices or slower devices using the thermo-optic (TO) effect. Hydrogenated amorphous silicon deposited by Plasma-Enhanced Chemical Vapor Deposition (PECVD) is a low loss material that has been used in multilayer stacks[3], but sufficient and stable hydrogenation of the silicon dangling bonds are critical to maintaining its low loss property. Zhu et al have demonstrated that the propagation loss for hydrogenated amorphous silicon waveguides starts to increase rapidly at temperatures above 300°C [4], and Selvaraja et al have shown that the refractive index change measured from a

Optoelectronic Interconnects XIII, edited by Alexei L. Glebov, Ray T. Chen, Proc. of SPIE Vol. 8630, 863012 · © 2013 SPIE · CCC code: 0277-786/13/$18 · doi: 10.1117/12.2005720

Mach-Zehnder Interferometer (MZI) starts to occur at 200°C [5]. In addition to thermal stability of hydrogenated amorphous silicon, another significant challenge is that the charge mobility is very low due to the amorphous structure of the film, thereby limiting its application in high-speed applications.

Deposition of polycrystalline silicon (polysilicon) is a mature, CMOS compatible process that is easy to deposit on a variety of substrates. In addition, it can be easily doped to realize electrically active photonic devices due to its relatively high (~100cm2/V-s) [6] electronic carrier mobility. Propagation loss has remained a significant challenge for polysilicon waveguides, which is dominated by scattering and absorption at the polycrystalline grain boundaries. Low loss (~6.45dB/cm) single mode polysilicon waveguides, [7, 8] high quality factor ring resonators [9], and high speed electro-optic modulators [10] formed by Solid Phase Crystallization (SPC) of Low Pressure Chemical Vapor Deposition (LPCVD) amorphous silicon have been demonstrated. Compared to direct deposition of LPCVD polysilicon, SPC of LPCVD amorphous silicon yields superior film qualities, such as smoother surfaces to reduce interfacial scattering and larger grains that result in fewer absorbing and scattering boundaries, further lowering the propagation loss [11].

To date, photonic polysilicon research has focused on waveguides and devices in the single mode region with thicknesses of 200-250nm and widths of 300-500nm, where narrower waveguides result in lower loss due to less confinement of light in the polysilicon core, indicating that attenuation is dominated by bulk loss [7]. Indeed, efforts to further reduce the overlap of the optical mode with the waveguide cross section have been made by forming polysilicon waveguides in the same step as the polysilicon transistor gate for electronics, resulting in core geometries of 120nm X 350nm and a propagation loss of 6.2 dB/cm at 1550nm [12]. Unfortunately, little work exists for wider, multimode polysilicon devices. Liao et al have reported that thicker and wider polysilicon waveguides suffer from higher propagation losses due to increased optical confinement [11]. However, for key photonic components such as multimode interference couplers (MMI) for beam splitting and arrayed waveguide gratings (AWG) for wavelength division multiplexing (WDM), device dimensions can span tens to hundreds of microns in width [13, 14]. Characterizing the loss of polysilicon at such widths is necessary to determine if these devices can be formed without prohibitively high losses.

In this paper, we demonstrate the lowest propagation loss to date of 0.56dB/cm to date in polysilicon waveguides, and experimentally confirm modal conversion due to polysilicon grain boundary scattering by examining the far field emission of a polysilicon grating coupler. In addition, we also demonstrate the first 1x12 polysilicon MMI with an insertion loss of -1.29dB and a uniformity of 1.07dB.

2. DESIGN AND FABRICATION

We have used the beam propagation method (BPM) from Rsoft to simulate 10μm wide waveguides for both crystalline silicon and polysilicon with grain boundaries, which is shown in Figure 2 (a) and (b), respectively. Figure 2(a) shows the 10μm wide crystalline silicon waveguide excited by the fundamental mode, which propagates through the waveguide undisturbed. In contrast, a polysilicon waveguide is simulated by adding grain boundaries. The grain boundaries scatter light into higher order modes that are still guided by the wide waveguide. For narrower waveguides, the grain boundaries scatter light into radiative modes, as higher order modes are not guided. Therefore, the number of guided modes in a given waveguide geometry determines the propagation loss due to grain boundary scattering.

In order to investigate the effect of the waveguide width on the propagation loss of polysilicon waveguides, the waveguide width is varied by using the structure shown in Figure 2(a). Grating couplers are used for input and output coupling. Due to the phase matching condition for grating couplers, the higher order modes excited by polysilicon grain boundary scattering will diffract out at different angles due to their different propagation constants. The details of this grating coupler will be reported separately. After the grating coupler, we first adiabatically taper all waveguide widths to 500 nm in order to filter out higher order modes and achieve single mode propagation. The waveguide is then adiabatically tapered to the desired waveguide width, which ranges from 400 nm to 10 μm. After 5 mm of propagation, all waveguides are then tapered back to the output waveguide width. The same structures are also fabricated on crystalline silicon as a reference. By having the exact same structure and fabrication process, our results can only arise from the differences between the two materials.

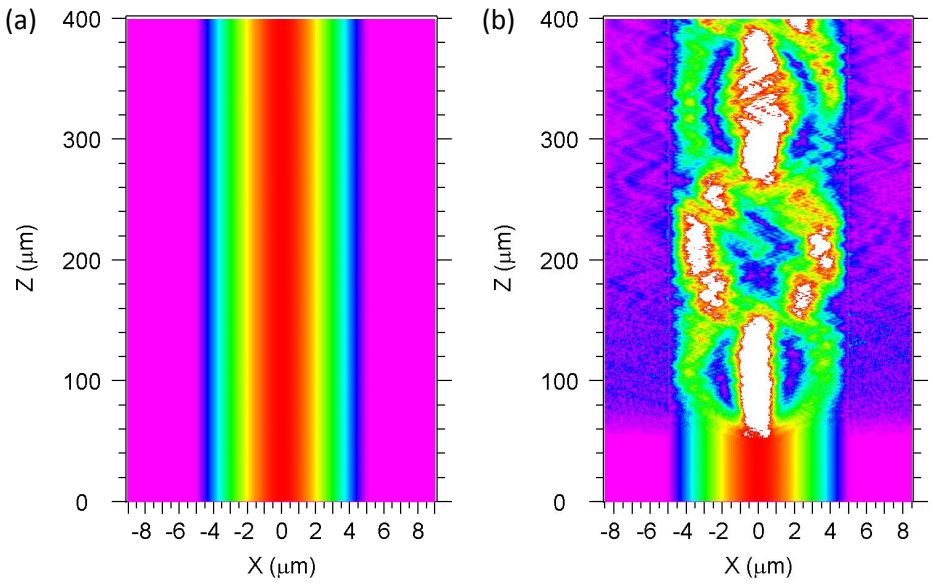

Figure 1-Beam Propagation Method simulation of 10μm waveguide for (a) crystalline silicon and (b) polysilicon with grain boundaries.

In addition, we also designed a 1x12 Multimode Interference (MMI) optical beam splitter to further demonstrate large multimode polysilicon devices. The length and width of the multimode region are L_{MMI}=563.4 μm and W_{MMI}=60 μm respectively. The input and access waveguides are both 2.6 μm wide. To clearly resolve the individual output spots in the near field, a fanout design was used to separate the 12 MMI output channels to 30 μm. A schematic of the 1x12 MMI can be seen in Figure 2(b).

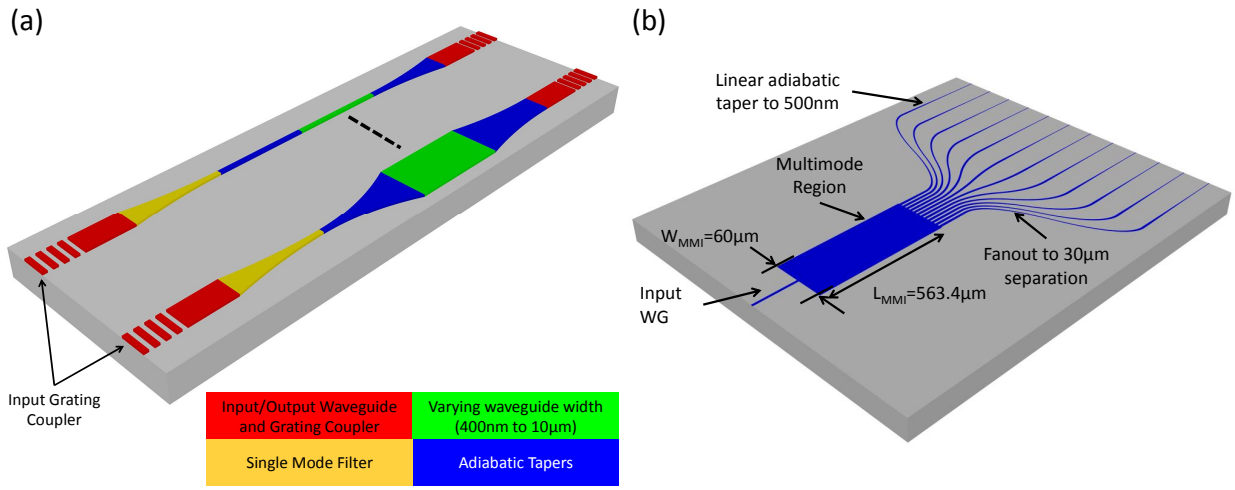

Figure 2-(a) Schematic of waveguide structure. Not drawn to scale. (b) Schematic of 1x12 polysilicon MMI.

In our experiment, we thermally oxidize a bare silicon wafer to create 2.0μm of SiO_2 which acts as the BOX layer and is thick enough to prevent optical leakage into the substrate. Afterwards, a 250nm thick layer of amorphous silicon was deposited using Low Pressure Chemical Vapor Deposition (LPCVD) at 550°C. From [15], we find that the deposition rate should be sufficiently high to minimize the number of nucleation sites, which results in increased grain size. Consequently, we use an increased silane gas flow of 150sccm to achieve a deposition rate of 3.3nm/minute. After the

amorphous silicon deposition, we briefly dip the wafers in Piranha solution to form a native oxide layer. This thin native oxide layer stabilizes the top surface of the amorphous silicon and prevents increased surface roughness during future anneal treatments [16]. The wafers are then annealed using a two-step annealing process. The first anneal is a low temperature anneal that is done at 600°C N_2 for 40 hours, and the purpose of this anneal is for gradual grain nucleation, which results in large grains. The second anneal is a 5 hour 1000°C also in N2, and this step is to crystallize the individual polysilicon grains.

In order to estimate our grain size, we use dry oxidation at 900°C for 30 minutes to oxidize the top surface of our polysilicon film. Because polysilicon grains will preferentially oxidize along grain boundaries, we can use Buffered Oxide Etch (BOE) to remove the oxide and then use Scanning Electron Microscopy (SEM) to visualize our grains. A picture of such an SEM image is shown in Figure 3(a), and we estimate the grain sizes to be ~300nm.

The waveguides were patterned using electron beam lithography and Reactive Ion Etching (RIE). Afterwards, a 1µm thick film of SiO2 for top cladding was deposited using PECVD. A cross section view of a single mode polysilicon waveguide is shown in Figure 3(b), and a microscope image of the 1x12 MMI is shown in Figure 3(c).

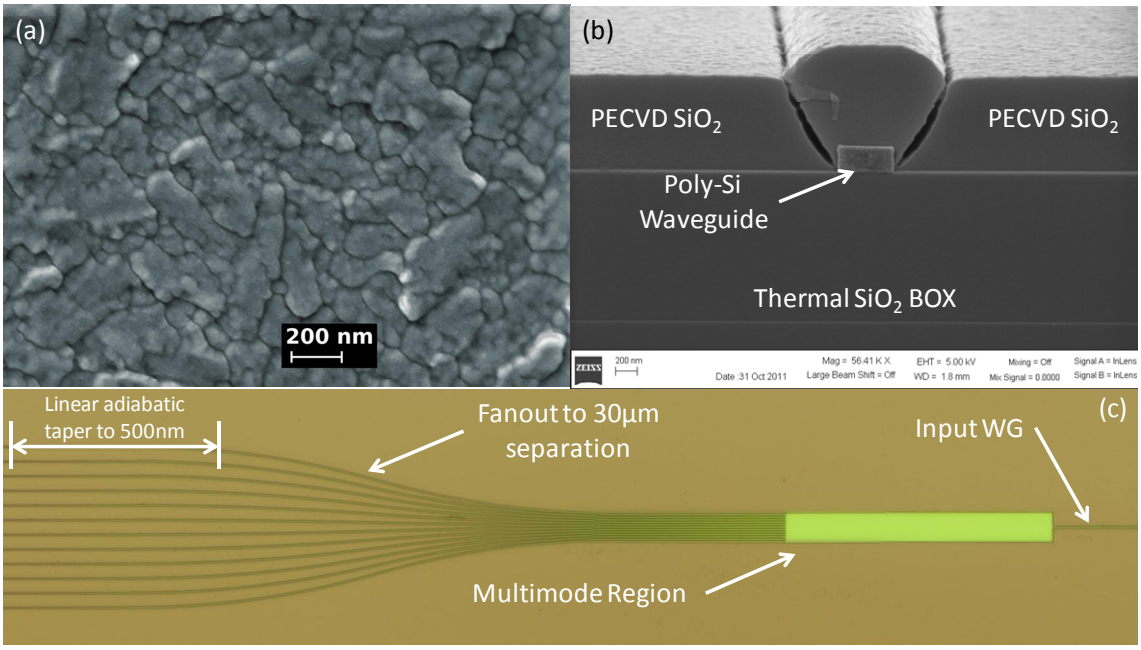

Figure 3-(a) Top down SEM image of polysilicon grains after oxidation and BOE, (b) cross sectional SEM of a single mode polysilicon waveguide and (c) microscope image of the completed 1x12 MMI.

3. RESULTS AND ANALYSIS

Transverse Electric (TE) polarized light at 1550nm was coupled into the input grating coupler using a polarization maintaining fiber (PMF) and collected from the output grating by standard single mode fiber (SMF). The propagation loss of various waveguide widths for both crystalline and polysilicon are shown below in Figure 4.

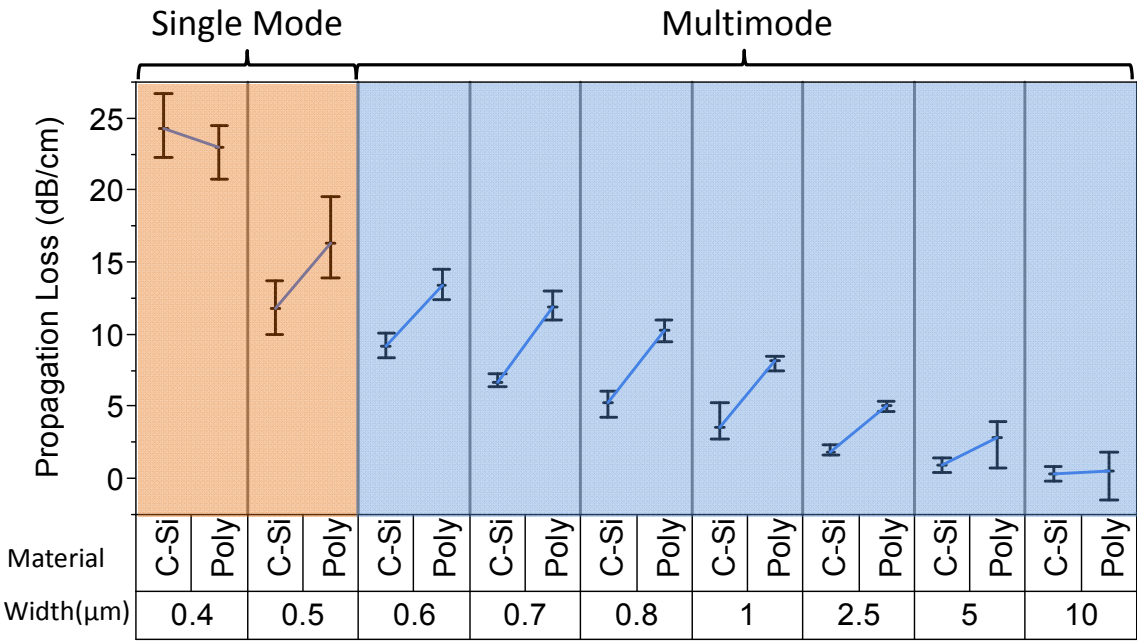

Figure 4-Propagation loss of various polysilicon and crystalline silicon waveguide widths.. Standard error bars are given for each data measurement.

The propagation loss decreases for both crystalline silicon and polysilicon as the waveguide width increases. At a waveguide width of 400nm, the propagation losses of crystalline and polysilicon are virtually the same, but as the waveguide width increases, the loss difference between the two also increases. For waveguide widths above 2.5µm, the difference in propagation loss between crystalline and polysilicon decreases until they have nearly identical propagation losses at 10µm. For crystalline silicon, this behavior is well known and is due to decreasing sidewall interaction of the fundamental mode of the waveguide [17]. However, the grain boundaries present in polysilicon cause scattering to either radiation modes or higher order modes depending on whether the waveguide width supports the higher modes. This scattering into radiation modes causes the additional loss between polysilicon and crystalline waveguides of the same width.

The presence of the higher order modes has been experimentally confirmed using the setup shown in Figure 5 (a) in which light at 1550nm is coupled out of the grating coupler and the far field image is observed on the IR CCD suspended 5cm above the grating. The higher order modes that are excited by the grain boundaries and can still be guided by the waveguide will have different propagation constants, and therefore will be emitted from the grating coupler at different angles according to the phase matching condition. The far field image for a crystalline silicon waveguide and grating can be seen in Figure 5(a), in which a single peak can be seen, which is due to only the fundamental mode of the waveguide being emitted. This can be contrasted with the far field of a polysilicon waveguide and grating with identical dimensions to that of crystalline silicon, which is shown in Figure 5(b). It can clearly be seen that there is not a single peak, but instead continuous emission across a multitude of angles, which indicates the presence of higher order modes each with their different propagation constants, and hence different emission angles. Such a result experimentally demonstrates the existence of mode conversion due to polysilicon grain boundary scattering.

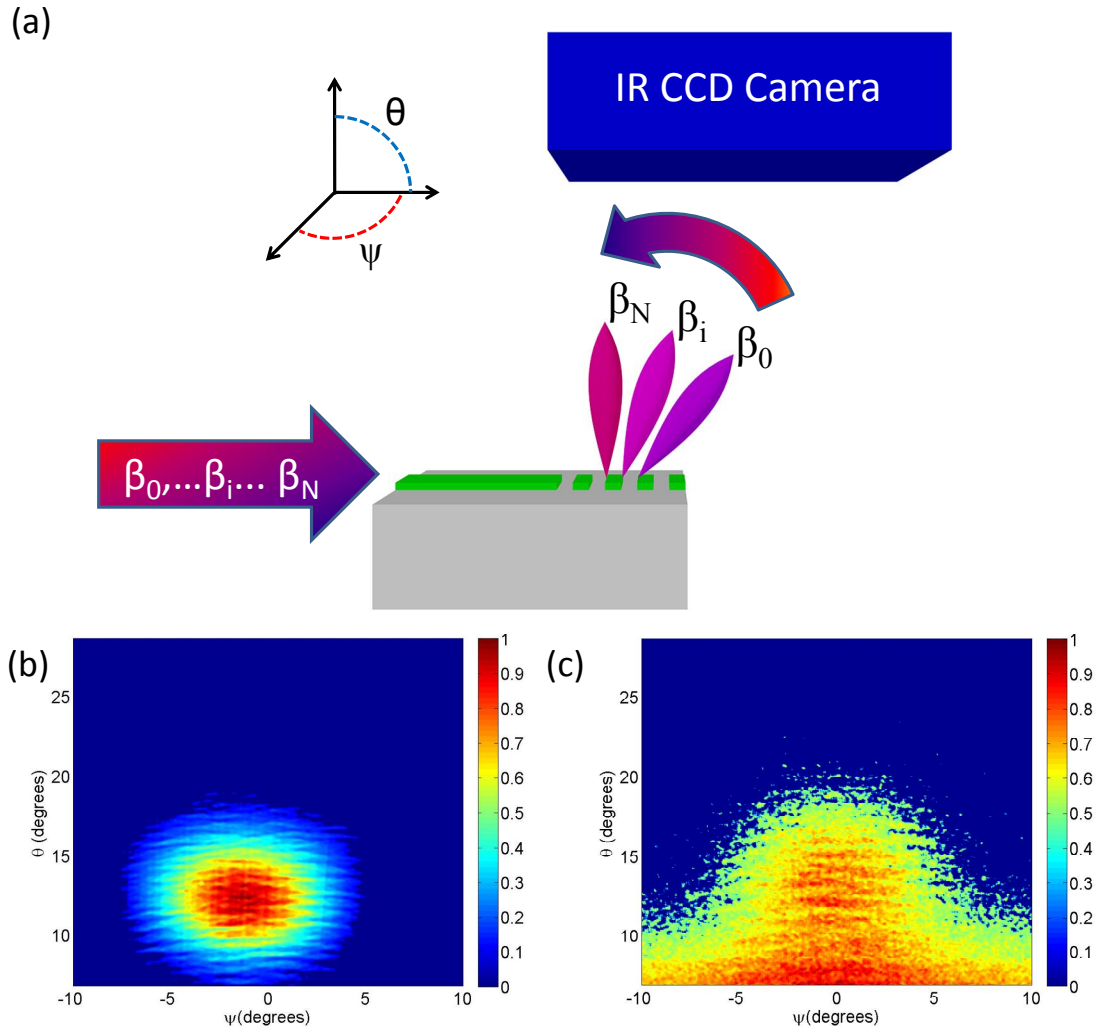

Figure 5-(a) Schematic of experimental setup using an IR CCD to examine the far field emission of the grating coupler. (b) Far field image of a crystalline waveguide and grating. (c) Far field image of polysilicon waveguide and grating identical to that made of crystalline silicon.

It is important to note that at a 10μm waveguide width, both polysilicon and crystalline silicon waveguides have the lowest losses of 0.56dB/cm and 0.31dB/cm, respectively. To our knowledge, this value is the lowest propagation loss for a polysilicon waveguide to date. Furthermore, it indicates that there is very little bulk absorption from the polysilicon grain boundaries. This behavior of decreasing propagation loss with increasing waveguide width validates the use of large polysilicon waveguides in photonic integrated circuits whenever bandwidth-density is affordable [18].

We fabricated the first polysilicon based 1x12 MMI and experimentally confirmed the functionality of such a 60μm wide polysilicon device. As before, TE polarized light at 1550nm was coupled into the 1x12 MMI. Using an IR camera, 12 output spots are imaged from the MMI fanout, which are shown in Figure 6(a). To characterize the performance of this 1x12 MMI, we used standard SMF to collect each of the 12 output intensities from the output grating couplers, which is shown in Figure 6(b). The performance of an MMI can be described by output uniformity and insertion loss. The uniformity is calculated as $10\log(I_{\max}/I_{\min})$, where I_{max} and I_{min} are the maximum and minimum output intensities of the MMI, respectively. The insertion loss of the MMI is defined as $-10\log(\sum I_i/I_{in})$, where I_i is the output intensity of the i^{th} output channel, and I_{in} is the intensity of a straight waveguide with the same dimensions of the MMI input waveguide. For our polysilicon 1x12 MMI, we determine a uniformity of 1.07dB and an insertion loss of -1.29dB.

This is due to the presence of the multimode region of the MMI, which is 60µm wide and 563.4µm long and has a much lower loss compared to the much narrower input waveguide. We have previously demonstrated a 1x12 MMI on crystalline silicon with comparable performance [19].

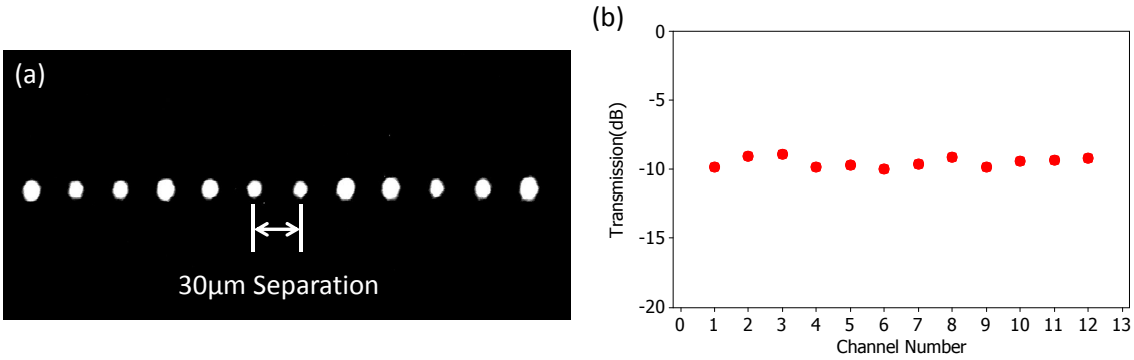

Figure 6-(a) IR image of the 12 output spots from 1x12 MMI fanout. (b) Output intensities of the 1x12 polysilicon MMI.

4. CONCLUSION

We have investigated the feasibility of multimode polysilicon waveguides to demonstrate the suitability of polysilicon as a candidate for multilayer photonic applications. SPC with a maximum temperature of 1000°C is used to create polysilicon on thermal SiO_2. We then measure the propagation losses for various waveguide widths on both polysilicon and crystalline silicon platforms. We find that as the width increases for polysilicon waveguides, the propagation loss decreases similarly to crystalline silicon waveguides. The difference in loss between the two platforms for a given waveguide width is due to the scattering from the polysilicon grain boundaries, which excites higher order modes. Depending on the waveguide width, these modes either propagate as higher order modes or are lost as radiation modes. Mode conversion due to grain boundary scattering is experimentally confirmed by observing the far field image of the grating coupler, in which the higher order modes are emitted at different angles according to their different propagation constants. We also find that at a waveguide width of 10µm, the polysilicon propagation loss of 0.56dB/cm is very close to the crystalline silicon propagation loss of 0.31dB/cm, indicating that there is little bulk absorption from the polysilicon. This result validates the use of polysilicon waveguides in photonic integrated circuits. We further demonstrate this with a 1x12 polysilicon MMI that has a low insertion loss of -1.29dB and a high uniformity of 1.07dB. Together, we present the lowest propagation loss for polysilicon waveguides to date of 0.56dB/cm as well as the first 1x12 polysilicon MMI.

Acknowledgements

This research is supported by the Multi-disciplinary University Research Initiative (MURI) program through the AFOSR, Contract No. # FA 9550-08-1-0394.

REFERENCES

[1] Nicolás Sherwood-Droz and Michal Lipson, "Scalable 3D dense integration of photonics on bulk silicon," Opt. Express **19**, 17758-17765 (2011).

[2] C. W. Holzwarth, J. S. Orcutt, H. Li, M. A. Popovic, V. Stojanovic, J. L. Hoyt, R. J. Ram, and H. I. Smith, "Localized Substrate Removal Technique Enabling Strong-Confinement Microphotonics in Bulk Si CMOS Processes," in Conference on Lasers and Electro-Optics/Quantum Electronics and Laser Science Conference and Photonic Applications Systems Technologies, OSA Technical Digest (CD) (Optical Society of America, 2008), paper CThKK5.

[3] JoonHyun Kang, Yuki Atsumi, Manabu Oda, Tomohiro Amemiya, Nobuhiko Nishiyama and Shigehisa Arai, "Low-Loss Amorphous Silicon Multilayer Waveguides Vertically Stacked on Silicon-on-Insulator Substrate," Jpn. J. Appl. Phys. **50,** 120208 (2011).

[4] Shiyang Zhu, G. Q. Lo, and D. L. Kwong, "Low-loss amorphous silicon wire waveguide for integrated photonics: effect of fabrication process and the thermal stability," Opt. Express **18**, 25283-25291 (2010).
[5] Shankar Kumar Selvaraja, Wim Bogaerts, Dries VanThourhout, and Marc Schaekers, "Thermal trimming and tuning of hydrogenated amorphous silicon nanophotonic devices," Appl. Phys. Lett. **97**, 071120 (2010).
[6] T. Kamins, Polycrystalline Silicon for Integrated Circuits and Displays, 2nd ed. (Kluwer, 1998).
[7] Shiyang Zhu, Q. Fang, M. B. Yu, G. Q. Lo, and D. L. Kwong, "Propagation losses in undoped and n-doped polycrystalline silicon wire waveguides," Opt. Express **17**, 20891-20899 (2009).
[8] Q. Fang, J. F. Song, S. H. Tao, M. B. Yu, G. Q. Lo, and D. L. Kwong, "Low loss (~6.45dB/cm) sub-micron polycrystalline silicon waveguide integrated with efficient SiON waveguide coupler," Opt. Express **16**, 6425-6432 (2008).
[9] Kyle Preston, Bradley Schmidt, and Michal Lipson, "Polysilicon photonic resonators for large-scale 3D integration of optical networks," Opt. Express **15**, 17283-17290 (2007).
[10] Kyle Preston, Sasikanth Manipatruni, Alexander Gondarenko, Carl B. Poitras, and Michal Lipson, "Deposited silicon high-speed integrated electro-optic modulator," Opt. Express **17**, 5118-5124 (2009).
[11] L. Liao, D. R. Lim, A. M. Agarwal, X. Duan, K. K. Lee, and L. C. Kimerling, "Optical transmission losses in polycrystalline silicon strip waveguides: effects of waveguide dimensions, thermal treatment, hydrogen passivation, and wavelength," J. Electron. Mater. **29**(12), 1380–1386 (2000).
[12] Jason S. Orcutt, Sanh D. Tang, Steve Kramer, Karan Mehta, Hanqing Li, Vladimir Stojanović, and Rajeev J. Ram, "Low-loss polysilicon waveguides fabricated in an emulated high-volume electronics process," Opt. Express **20**, 7243-7254 (2012).
[13] Hosseini, A.; Kwong, D.N.; Yang Zhang; Subbaraman, H.; Xiaochuan Xu; Chen, R.T., "1xN multimode interference beam splitter design techniques for on-chip optical interconnections," IEEE Jounal of Selected Topics in Quantum Electronics **17**, 510-515 (2011).
[14] P. Dumon, W. Bogaerts, D. Van Thourhout, D. Taillaert, R. Baets, J. Wouters, S. Beckx, and P. Jaenen, "Compact wavelength router based on a Silicon-on-insulator arrayed waveguide grating pigtailed to a fiber array," Opt. Express **14**, 664-669 (2006).
[15] Hatalis, Miltiadis K.; Greve, David W.; , "Large grain polycrystalline silicon by low-temperature annealing of low-pressure chemical vapor deposited amorphous silicon films," Journal of Applied Physics, **63,** 2260-2266, (1988).
[16] Effiong Ibok and Shyam Garg, "A Characterization of the Effect of Deposition Temperature on Polysilicon Properties," J. Electrochem. Soc. **140**, 2927 (1993).
[17] Yurii Vlasov and Sharee McNab, "Losses in single-mode silicon-on-insulator strip waveguides and bends," Opt. Express **12**, 1622-1631 (2004).
[18] Mauro J. Kobrinsky, Bruce A. Block, Jun-Fei Zheng, Brandon C. Barnett, Edris Mohammed, Miriam Reshotko, Frank Robertson, Scott List, Ian Young, Kenneth Cadien, "On-Chip Optical Interconnects," Intel Technology Journal, **8**, 129-142 (2004).
[19] Kwong, D.; Zhang, Y.; Hosseini, A.; Liu, Y.; Chen, R.T.; , "1 X 12 even fanout using multimode interference optical beam splitter on silicon nanomembrane," Electronics Letters, **46**, 1281-1283 (2010).